Coupled simulations of RF feedback stabilization of tearing modes

Scott E. Kruger[a], Thomas G. Jenkins[a], Eric D. Held[b], Jesus J. Ramos[c], R.W. Harvey[d] Dalton D. Schnack[e],

a) Tech–X Corporation, 5621 Arapahoe Avenue Suite A, Boulder, Colorado, 80303

b) Utah State University, Logan, Utah, 84322

c) Massachusetts Institute of Technology, Cambridge, Massachusetts, 02139 d) CompX Corporation, Del Mar, CA 92014-5672

e) University of Wisconsin, Madison, Wisconsin, 53706

Abstract

A model which incorporates the effects of electron cyclotron current drive (ECCD) into the magnetohydrodynamic (MHD) equations is implemented in the NIMROD code [C. R. Sovinec *et al.*, J. Comp. Phys. **195**, 355 (2004)] and used to investigate the effect of ECCD injection on the stability, growth, and dynamical behavior of magnetic islands associated with resistive tearing modes. Predictions of the model are shown to quantitatively and qualitatively agree with numerical results obtained from the inclusion of localized ECCD deposition in static equilibrium solvers. The complete suppression of the $(2, 1)$ resistive tearing mode by ECCD is demonstrated. Consequences of the shifting of the mode rational surface in response to the injected current are explored, as are the consequences of spatial ECCD misalignment. We discuss the relevance of this work to the development of more comprehensive predictive models (in support of existing/future experiments, e.g. ITER) for ECCD–based mitigation and control of neoclassical tearing modes.

1 Introduction

Electron cyclotron current drive (ECCD) has successfully been used to stabilize tearing modes in multiple experiments [1, 2, 3, 4]. Such experiments may rely on sophisticated active feedback control to locate and drive time–modulated current in island O–points of the rotating plasma [4, 5, 6]; alternatively, continuously driven current whose spatial alignment is tailored to yield a net stabilizing effect on the mode may be employed [4, 7, 8]. Using these two approaches, considerable efforts have been made to determine an optimal strategy for the mitigation and control of magnetic islands in the ITER device [9, 10]. Initial theoretical calculations relevant to the suppression and control of NTMs [11, 12, 13] have also demonstrated that localized ECRH or ECCD applied at the O–point of magnetic islands can reduce island saturation widths. These analytic results explore the ECRF-induced modifications to the Rutherford equation [14], and emphasize the importance of localization of the driven current within the magnetic island for the most efficient stabilization of the tearing modes. If the driven current is perfectly localized, then currents less than one percent of the plasma current are needed to stabilize the modes. Current work includes adding a synthetic control system for studying the effects of the modes.

2 Mathematical Formulation of Computational Approach

Computational efforts in the modeling of ECCD stabilization in MHD codes can be roughly generalized into two groups, depending on the complexity of the model. In the first group [15, 16, 17, 18], the current source is given by modifying the resistive Ohm's law,

$$\mathbf{E} + \mathbf{u} \times \mathbf{B} = \frac{\eta}{\mu_0} \left(\mathbf{J} - \mathbf{J}_{RF} \right) \ , \tag{1}$$

and various heuristic models for the current driven by the applied electric field are employed. In the second group of simulations [19, 20], the basic model of Eq. (1) for the driven current is retained, but reduced MHD equations are used (in which the dynamics of compressional Alfvén waves is not retained). An auxiliary drag/diffusion equation for the RF source is also added to equilibrate the current. In this way, the parallel and perpendicular transport of the electrons that are driven by the RF sources can be modeled;

$$\frac{\partial J_{RF}}{\partial t} = \nabla \cdot (\chi_{\parallel} \nabla_{\parallel} J_{RF}) + \nabla \cdot (\chi_{\perp} \nabla_{\perp} J_{RF}) + \nu (J - J_{RF}) \tag{2}$$

This model is heuristically derived based on the Fokker-Planck equation, and we will refer to it as the Giruzzi model [21].

Rigorously, the mathematical formulation of how ECCD sources can be incorporated into a fluid model relies on the observation [22] that ECCD only slightly modifies the distribution function; thus, the induced distortion of the distribution function away from Maxwellian is on the same order as the distortions required to calculate the stress tensors, heat fluxes, and collisional frictions used to close the fluid moments. The procedure outlined in Ref. [22] develops the equation for the kinetic distortion in terms of a Chapman-Enskog-like closure [23]. Ramos improved this formalism to more rigorously include the drift effects required to obtain the bootstrap current form [24]. The numerical implementation of the closure scheme will be discussed later. In the simulations presented in the next section, we will set the closure terms to zero; a discussion of where the RF-induced physics appears in the fluid moment model will elucidate the strengths and weaknesses of this approach.

Inclusion of the physics of RF waves into low-order moment equations is a multiscale problem. To proceed, the

high-frequency RF fields and the consequent plasma response are separated from the slower spatiotemporal evolution:

$$\begin{aligned} f_\alpha(\mathbf{x},\mathbf{v},t) &= \langle f_\alpha\rangle_{MHD}(\mathbf{x}_{MHD},\mathbf{v}_{MHD},t_{MHD}) \\ &\quad + \epsilon f_{\alpha RF}(\mathbf{x}_{MHD},\mathbf{v}_{MHD},t_{MHD},\mathbf{x}_{RF},\mathbf{v}_{RF},t_{RF}), \\ \mathbf{E}(\mathbf{x},t) &= \langle\mathbf{E}\rangle_{MHD}(\mathbf{x}_{MHD},t_{MHD}) + \epsilon\mathbf{E}_{RF}(\mathbf{x}_{MHD},t_{MHD},\mathbf{x}_{RF},t_{RF}), \\ \mathbf{B}(\mathbf{x},t) &= \langle\mathbf{B}\rangle_{MHD}(\mathbf{x}_{MHD},t_{MHD}) + \epsilon\mathbf{B}_{RF}(\mathbf{x}_{MHD},t_{MHD},\mathbf{x}_{RF},t_{RF}), \end{aligned} \tag{3}$$

where $\langle\ldots\rangle$ denotes an average over the RF time and spatial scales. The RF terms are annihilated with this operator; the averaged kinetic equation thus represents the familiar kinetic equation applicable at MHD spatiotemporal scales, along with a new term:

$$\frac{\partial\langle f_\alpha\rangle_{MHD}}{\partial t} + \mathbf{v}_{MHD}\cdot\vec{\nabla}\langle f_\alpha\rangle_{MHD} + \frac{q_\alpha}{m_\alpha}\left[\langle\mathbf{E}\rangle_{MHD} + \mathbf{v}_{MHD}\times\langle\mathbf{B}\rangle_{MHD}\right]\cdot\vec{\nabla}_{\mathbf{V}}\langle f_\alpha\rangle_{MHD} \tag{4}$$

$$+\left\langle\frac{q_\alpha}{m_\alpha}\left[\mathbf{E}_{RF} + \mathbf{v}\times\mathbf{B}_{RF}\right]\cdot\vec{\nabla}_{\mathbf{V}} f_{\alpha RF}\right\rangle = C(\langle f_\alpha\rangle_{MHD}) \tag{5}$$

The RF term represents the beating of a high-frequency RF wave and a nearly-commensurate, RF-induced high-frequency perturbation to the distribution function; the ensuing beat frequencies are thus considerably higher/lower than the characteristic RF frequency. While the high-frequency beating effects are inconsequential, the low-frequency effects are comparable to characteristic MHD frequencies; thus, although this term is of order ϵ^2, it must be retained.

The procedure to find this term is the quasilinear theory that is described in Stix [25]. Briefly, equations of order ϵ^0 describe the evolution of MHD density, temperature, and flow velocity profiles at lowest order, while the order ϵ equations describe the linear propagation of RF waves through these MHD profiles. Windowed Fourier transforms are used to solve the latter equations at this order, and the resultant expressions for RF-induced fields and distribution functions can then be put back into the new source term in the kinetic equations. Upon averaging over RF spatiotemporal scales, this term becomes a quasilinear diffusion operator. Dropping the MHD subscripts and averaging operator, we have:

$$\frac{\partial f_\alpha}{\partial t} + \mathbf{V}\cdot\vec{\nabla} f_\alpha + \frac{q_\alpha}{m_\alpha}\left[\mathbf{E} + \mathbf{v}\times\mathbf{B}\right]\cdot\vec{\nabla} f_\alpha = C(f_\alpha) + Q_{rf}(f_\alpha) \tag{6}$$

where $Q_{rf}(f_\alpha)$ is the quasilinear operator, the moments of which will be shown below.

Derivation of the fluid equations can either be carried out by taking moments of the kinetic equation and then ordering to obtain a closure, or (as has more recently been shown) by ordering the kinetic equation directly to obtain a drift-kinetic equation and then calculating moments and closures [26, 24]. The fluid equations can be written as [26, 24, 22]:

$$\frac{\partial\rho}{\partial t} + \nabla\cdot(\rho\mathbf{u}) = 0\,, \tag{7}$$

$$\rho\frac{\partial\mathbf{u}}{\partial t} + \rho(\mathbf{u}\cdot\nabla)\mathbf{u} = -\nabla p + \mathbf{J}\times\mathbf{B} - \nabla\cdot\overleftrightarrow{\mathbf{\Pi}}, \tag{8}$$

$$\mathbf{E} + \mathbf{u}\times\mathbf{B} = \mathbf{R}_e + \frac{1}{ne}\left[\mathbf{J}\times\mathbf{B} - \vec{\nabla}(p_e) - \vec{\nabla}\cdot\mathbf{\Pi} + \mathbf{F}_e^{rf}\right]\,, \tag{9}$$

$$\frac{3}{2}n\alpha\left(\frac{\partial T_\alpha}{\partial t} + (\mathbf{u}_\alpha\cdot\nabla)T_\alpha\right) + p_\alpha\nabla\cdot\mathbf{u}_\alpha = -\nabla\cdot\mathbf{q}_\alpha - \overleftrightarrow{\mathbf{\Pi}}_\alpha\colon\nabla\mathbf{u}_\alpha + Q_\alpha + S_\alpha^{rf}\,, \tag{10}$$

along with the pre-Maxwell equations:

$$\nabla\times\mathbf{B} = \mu_0\mathbf{J}\,;\;\; \nabla\cdot\mathbf{B} = 0\,;\;\; \nabla\times\mathbf{E} = -\frac{\partial\mathbf{B}}{\partial t}\,. \tag{11}$$

The closures include the higher-order moments

$$\mathbf{q}_\alpha^{rf} = \int m_\alpha \mathbf{v} f_\alpha d\mathbf{v} \; ; \; \mathbf{\Pi}_\alpha^{rf} = \int m_\alpha \mathbf{v}_\alpha \mathbf{v}_\alpha f_\alpha d\mathbf{v} \; , \tag{12}$$

with collisional moments

$$\mathbf{R}_e^{rf} = \int m_e \mathbf{v} C(f_\alpha) d\mathbf{v} \; ; \; Q_e^{rf} = \int \frac{m_e v^2}{2} C(f_\alpha) d\mathbf{v} \; , \tag{13}$$

and the quasilinear moments

$$\mathbf{F}_e^{rf} = \int m_e \mathbf{v} Q_{rf}(f_\alpha) d\mathbf{v} \; ; \; S_e^{rf} = \int \frac{m_e v^2}{2} Q_{rf}(f_\alpha) d\mathbf{v} \; , \tag{14}$$

To obtain these closures, a CEL-like formalism [23] is used. The entire equation for the kinetic closure may be found in Ref. [24], but here we note that the RF terms also drive the kinetic distortion:

$$\frac{dF_e}{dt} - C(f_M + F_e) = \cdots + Q(f_M) - \frac{\mathbf{v} \cdot \mathbf{F}_e^{RF}}{T} f_M - \frac{2}{3} \frac{S_e^{RF}}{nT} \left[\frac{mv^2}{2T} - \frac{3}{2} \right] f_M \tag{15}$$

RF physics is typically explained in terms of a simplified kinetic equation called a Fokker-Planck equation [27]. For analytic studies, these equations are typically as simple as possible to clarify the qualitative physics of RF processes; however, modern Fokker-Planck codes use bounce-averaged drift-kinetic equations which also contain the quasilinear terms [28, 29]. Our above drift-kinetic equation contains the physics needed for describing ECCD current drive.

Before discussing how RF physics enters into the fluid approach, we wish to discuss the collisional friction in particular. Using a moment approach, this term can be written as [30]:

$$\mathbf{R}_{ei} = \eta \left[\mathbf{J} + \frac{3e\mathbf{q}_e}{5T_e} \right] \tag{16}$$

Thus, even in the absence of RF physics, the closure physics can be seen to affect the resistivity in the Spitzer problem. As discussed in Refs. [31, 27], the physics associated with the ECCD can be categorized into three distinct effects:

- Wave-electron parallel momentum exchange. This is represented by the F_e^{RF} term. This term drives only about a third of the total driven current of ECCD due to its resonance with the perpendicular component of the velocity. The time scale for this term is the time scale due to the gyrotron [32], which is on the order of $10 - 100\mu s$ and is dominantly determined by the time scale of the voltage supplies.

- Asymmetric collisionality. Because energy is deposited into the perpendicular component of the electron distribution function, the distortion gives an asymmetric resistivity that causes current to be driven. This is the Fisch-Boozer effect [33] and is the dominant mechanism for the current drive.

- Selective electron trapping. For resonant particles near the trapped-passing boundary, the energy deposited into the electrons can cause passing electrons to become trapped, thus decreasing the total current. This is the Ohkawa effect [34].

These terms are often termed "currents", in the same way the electron stress tensor term in the moment equation is termed the bootstrap current, because they all have collisional dependency similar to the $\eta\mathbf{J}$ term. However, the total plasma current (as defined by the integral over the current density) will rise on an inductive time scale.

The Fisch-Boozer current can be described using a drift kinetic equation without the drift terms [33]. Solutions of the kinetic distortion equation without the drift terms [23] show that the dominant effect is on the parallel heat

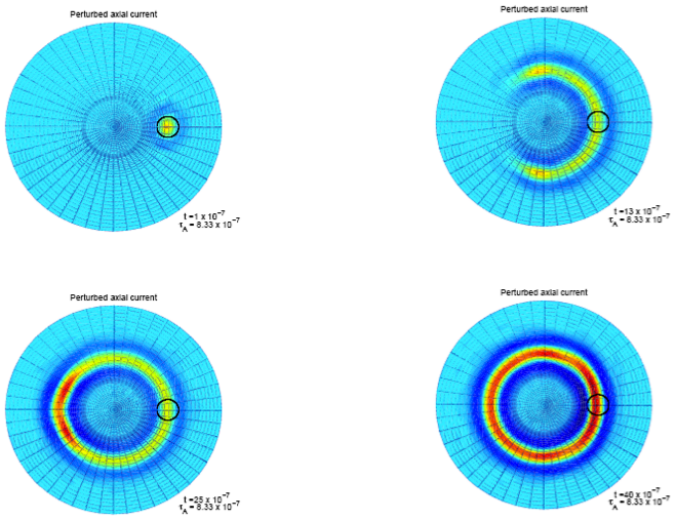

Figure 1: Compressional Alfvén waves equilibrate current sources, as demonstrated in this example in cylindrical geometry. From a poloidally localized source, the toroidal current density evolves to fill the surface in approximately 5 Alfvén times.

flux. This is consistent with the modifications of collisional friction occurring through heat flux modifications in the standard $\eta\mathbf{J}$ term (as seen in Eq. 16). The Ohkawa term is a modification of the trapped particle effects, and requires the inclusion of the drift terms in the drift kinetic equations, to obtain correctly [34, 27]. This is the DKE term required to give a correct calculation for the bootstrap current. Because the trapped particles will also reduce the parallel heat flux [35], the Ohkawa current requires the stress tensor and heat flux terms calculated from a drift kinetic equation that contains the correct drift terms [24].

The Giruzzi model for the coupled RF/MHD problem, therefore, can be viewed as a model for the stress tensor and heat flux effects with an emphasis on getting the time scales of the individual terms correct [31]. In the subsequent work, we will ignore the electron stress tensor, use a Braginskii closure for the parallel heat flux, and ignore the heat flux contributions to the resistivity. Although our source will be analytically specified in the next section, we will use a $tanh$ function with a fast time scale. This gives the same qualitative behavior as the Giruzzi model. For the equilibration along a field line, we rely on compressional Alfvén waves to equilibrate the sources instead of an explicit anisotropic operator. That this effectively equilibrates the sources is shown in Fig. 1.

3 Computational approach

The MHD dynamics of our simulations will be solved using the NIMROD code, the details of which will be discussed shortly. We must first return to the calculation needed to get the momentum and thermal source terms arising from the quasilinear operator. Beginning with the ordering shown in Eq. 3, the subsequent analysis for the quasilinear operator Fourier transforms the RF time and spatial scales (consistent with the eikenol approximation used for the ray

propagation). The source term then requires the following calculation:

$$S_e^{RF} = \frac{e^2 n_e i}{(2\pi)^{5/2} L^3 T_e} \iiiint \sum_{m=-\infty}^{\infty} \frac{|\psi|^2 e^{-m_e v_\parallel^2/2T_e} e^{-m_e v_\perp^2/2T_e} k_\perp v_\perp}{(v_{Te})^3 \left(\omega + i\gamma - k_\parallel v_\parallel - m\Omega_{ce}\right)} dk_\perp dk_\parallel dv_\perp dv_\parallel \tag{17}$$

wherein

$$\psi = E_{\parallel RF} v_\parallel J_m(z) + v_\perp (E_k + iE_\zeta)/2J_{m-1}(z) + +v_\perp (E_k - iE_\zeta)/2J_{m+1}(z) \ , \tag{18}$$

and we have $z = k_\perp v_\perp / \Omega_{ce}$ and $J_n(z)$ is the standard Bessel function.

The RF fields are calculated using the GENRAY code [36], which returns linear RF propagation data at a set of points along each ray. The rays are distributed according to a pattern that can be specified to model the antenna. In our work, we use a set of rays that begins as a set of concentric circles. As they propagate through the plasma, the ray trajectories will distort, ultimately leading to a set of points that are (at some level) spatially unstructured. To compute the quasilinear integrals, we must be concerned with not only the data along individual rays, but also with the collective behavior of the ray bundle; decreases in power flux along the path of the bundle correspond to deposited RF power in the plasma. Using an adequately large number of rays should yield numerical convergence, since increasing the ray count within a fixed volume yields both a lower power for each individual ray and a smaller area-perpendicular-to-flow through which this power must pass (thus maintaining a relatively constant contribution to the power flux). The relevant areas must be calculated; to do so, we use the QHULL [37] computational geometry software to take coplanar projections of the GENRAY points. These points constitute a grid from which a Voronoi (dual mesh) diagram can be calculated; the areas of the Voronoi cells are then easily computed. An example of the mesh calculated is shown in Fig. 2.

After the integration over the wave numbers is performed, velocity moments are taken to calculate the value of the quasilinear terms in real space (recall that the Fourier wavenumbers are only applicable to RF scale lengths). One now has the value of this term on the three-dimensional, unstructured GENRAY grid, and it is then necessary to interpolate it onto the NIMROD grid. NIMROD uses a high-order finite-element mesh for the poloidal plane and a pseudo-spectral method for the toroidal direction [38]; we consider each one in turn.

The magnitude of the quasilinear operator from the GENRAY ray bundle is superimposed on the poloidal mesh of NIMROD in Fig. 3. Even though the quasilinear source is highly localized, the NIMROD grid resolution can be increased relative to running without sources to adequately resolve this increased localization. In the figure, 421 GENRAY rays are shown. To interpolate the GENRAY data onto the NIMROD mesh, Shepard's algorithm [39], as given in the TOM's library [40], is used to interpolate the scattered data.

The toroidal discretization of the RF source term is more difficult to resolve. As seen in Fig. 4, even with 32 Fourier modes (corresponding to 32 discrete planes on which data can be deposited), peak RF deposition can occur between the colocation points (planes) used in NIMROD's pseudospectral method. To resolve this dataset, 512 Fourier modes would be needed, which is prohibitive for most runs. To more easily model the salient physics, we use the following approximation:

$$F_{RF}(R, Z, \phi) \approx \left[\oint_0^{2p} F_{RF}(R, Z, \phi) d\phi \right] g(\phi). \tag{19}$$

As discussed in Refs. [31, 19], the function $g(\phi)$ can also represent the effects of toroidal rotation. In those references, a square box was used. We use

$$g(\phi) = \frac{2\pi}{\phi_c} \cos\left(\frac{\pi(\phi - \phi_c)}{2\phi_c}\right)^2 ; \quad |\phi - \phi_c| \leq \phi_c \tag{20}$$

In addition to giving reasonable localization, this method avoids the Gibbs phenomena that unavoidably occur when one attempts to resolve a square box with a spectral method.

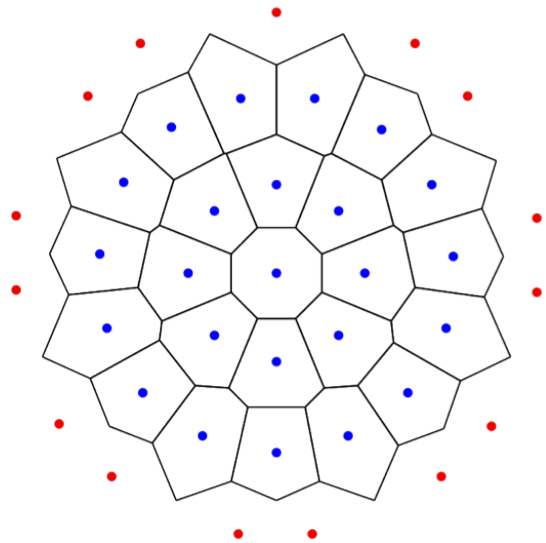

Figure 2: An example of the mesh created from the GENRAY data points (blue). Using the QHULL package, the Delaunay triangulation of this data (not shown) is constructed, and the outermost triangles are then reflected across the convex hull to form ghost points (shown in red). The Voronoi diagram (black) of the GENRAY and ghost datasets is then created, and the areas of Voronoi cells are calculated. Inclusion of ghost points ensures the finite area of the outermost Voronoi cells.

With the details of the calculation of the terms that enter the MHD equations described, we now explain the method of code coupling which enables the temporal evolution of our simulations. Rather than creating a single code with all of the needed physics, we opted for a paradigm of maintaining standalone executables and coupling the data via files. To enable this approach, we use the Integrated Plasma Simulator (IPS) framework [41] to enable the workflow composition shown in Fig. 5. NIMROD is run continuously, outputting its data in files at every 10 time steps (with each time step corresponding to $100\tau_A$). When the data file is written, the IPS framework detects it and executes a preprocessing program that translates the axisymmetric fields from NIMROD to a form that GENRAY can use as input. GENRAY then calculates the ray trajectories based on the $n = 0$ fields, and writes these trajectories and the corresponding electric fields to a file. A third program then reads this data and interfaces with QHULL to calculate the quasilinear operator. NIMROD then reads the quasilinear operator, takes the moments, and interpolates the sources onto the NIMROD grid. The temporal advance presented here is an explicit scheme: the sources are calculated based on fields that are older than the source update. However, the sources are updated typically within $2000\tau_A = 2\times10^{-4}s$, which is still less than the L/R time of $0.22\ s$ (over which the equilibrium is modified by the currents) so using an explicit scheme is justified.

Initial results of the simulations are shown in Fig. **??**. In this simulation, the TeX

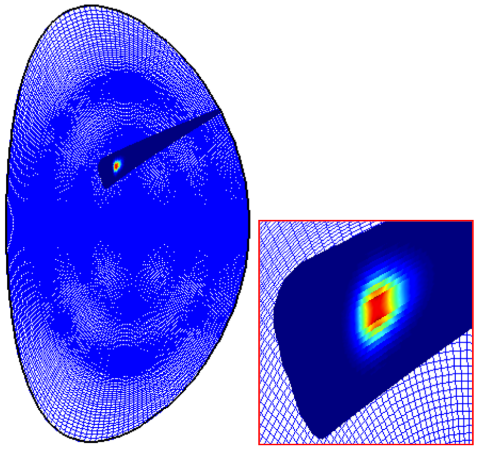

Figure 3: A plot of the magnitude of the quasilinear operator from the GENRAY ray bundle, superimposed on NIMROD's finite element mesh, shows the localized nature of the source.

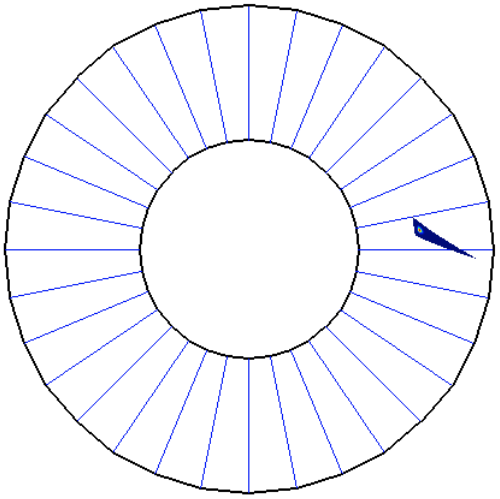

Figure 4: A plot of the magnitude of the quasilinear operator from the GENRAY ray bundle, superimposed on the poloidal planes corresponding to NIMROD's toroidal pseudospectral representation, shows the localized nature of the source.

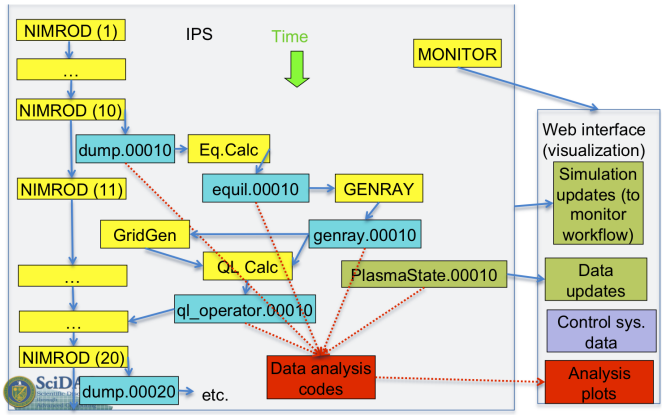

Figure 5: NIMROD and GENRAY are coupled together using the SWIM IPS framework, along with additional auxiliary routines for calculating the $n = 0$ equilibrium and the quasilinear operator.

References

[1] H. Zohm, G. Gantenbein, G. Giruzzi, S. Günter, F. Leuterer, M. Maraschek, J. P. Meskat, A. G. Peeters, W. Suttrop, and D. Wagner, "Experiments on neoclassical tearing mode stabilization by ECCD in ASDEX Upgrade," *Nuclear Fusion*, vol. 39, no. 5, pp. 577–580, 1999.

[2] G. Gantenbein, H. Zohm, G. Giruzzi, S. Günter, F. Leuterer, M. Maraschek, J. P. Meskat, Q. Yu, and A. Team, "Complete suppression of neoclassical tearing modes with current drive at the electron-cyclotron-resonance frequency in ASDEX Upgrade tokamak," *Physical Review Letters (ISSN 0031-9007)*, vol. 85, no. 6, pp. 1242–1245, 2000.

[3] A. Isayama, Y. Kamada, S. Ide, and K. Hamamatsu, "Complete stabilization of a tearing mode in steady state high-beta," *Plasma Physics and Controlled Fusion*, 2000.

[4] R. J. La Haye, S. Günter, D. A. Humphreys, J. Lohr, T. C. Luce, M. Maraschek, C. C. Petty, R. Prater, J. T. Scoville, and E. J. Strait, "Control of neoclassical tearing modes in DIII–D," *Physics of plasmas*, vol. 9, p. 2051, 2002.

[5] D. A. Humphreys, J. R. Ferron, R. J. La Haye, T. C. Luce, C. C. Petty, R. Prater, and A. S. Welander, "Active control for stabilization of neoclassical tearing modes," *Physics of plasmas*, vol. 13, no. 5, p. 056113, 2006.

[6] R. Prater, R. LaHaye, T. C. Luce, C. C. Petty, E. J. Strait, J. R. Ferron, D. A. Humphreys, A. Isayama, J. Lohr, K. Nagasaki, P. A. Politzer, M. R. Wade, and A. S. Welander, "Stabilization and prevention of the 2/1 neoclassical tearing mode for improved performance in DIII-D," *Nuclear Fusion*, vol. 47, pp. 371–377, Apr. 2007.

[7] A. Isayama, Y. Kamada, N. Hayashi, T. Suzuki, T. Oikawa, T. Fujita, T. Fukuda, S. Ide, H. Takenaga, K. Ushigusa, T. Ozeki, Y. Ikeda, N. Umeda, H. Yamada, M. Isobe, Y. Narushima, K. Ikeda, S. Sakakibara, K. Yamazaki, K. Nagasaki, and the JT-60 Team *Nucl. Fusion*, vol. 43, p. 1272, 2003.

[8] M. Maraschek, G. Gantenbein, Q. Yu, H. Zohm, S. Günter, F. Leuterer, and A. Manini, "Enhancement of the Stabilization Efficiency of a Neoclassical Magnetic Island by Modulated Electron Cyclotron Current Drive in the ASDEX Upgrade Tokamak," *Physical Review Letters (ISSN 0031-9007)*, vol. 98, no. 2, pp. 1–4, 2007.

[9] R. LaHaye, R. Prater, R. J. Buttery, N. Hayashi, A. Isayama, M. Maraschek, L. Urso, and H. Zohm, "Cross-machine benchmarking for ITER of neoclassical tearing mode stabilization by electron cyclotron current drive," *Nuclear Fusion*, vol. 46, pp. 451–461, Feb. 2006.

[10] N. Hayashi, T. Ozeki, K. Hamamatsu, and T. Takizuka, "ECCD power necessary for the neoclassical tearing mode stabilization in ITER," *Nuclear Fusion*, vol. 44, pp. 477–487, Mar. 2004.

[11] C. C. Hegna and J. D. Callen, "On the stabilization of neoclassical magnetohydrodynamic tearing modes using localized current drive or heating," *Physics of Plasmas*, vol. 4, no. 8, pp. 2940–2946, 1997.

[12] F. W. Perkins, R. W. Harvey, M. A. Makowski, M. N. Rosenbluth, S. ITER, and C. La Jolla, "Prospects for electron cyclotron current drive stabilization ofneoclassical tearing modes in ITER," *17th IEEE/NPSS Symposium Fusion Engineering, 1997*, vol. 2, 1997.

[13] H. Zohm, "Stabilization of neoclassical tearing modes by electron cyclotron current drive," *Physics of plasmas*, 1997.

[14] P. H. Rutherford *Phys. Fluids*, vol. 16, p. 1903, 1973.

[15] G. Kurita, T. Tuda, M. Azumi, T. Takizuka, and T. Takeda, "Effect of local heating on the m=2 tearing mode in a tokamak," *Nucl. Fusion*, vol. 34, p. 1497, Nov. 1994.

[16] E. Uchimoto, M. Cekic, R. W. Harvey, C. Litwin, S. C. Prager, J. S. Sarff, and C. R. Sovinec *Phys. Plasmas*, vol. 1, p. 3517, 1994.

[17] J. S. Sarff, A. F. Almagri, M. Cekic, C.-S. Chaing, D. Craig, D. J. D. Hartog, G. Fiskel, S. A. Hokin, R. W. Harvey, H. Ji, C. Litwin, S. C. Prager, D. Sinitsyn, C. R. Sovinec, J. C. Sprott, , and E. Uchimoto *Phys. Plasmas*, vol. 2, p. 2440, 1995.

[18] C. R. Sovinec and S. Prager *Nucl. Fusion*, vol. 39, p. 777, 1999.

[19] Q. Yu, S. Günter, G. Giruzzi, K. Lackner, and M. Zabiego, "Modeling of the stabilization of neoclassical tearing modes by localized radio frequency current drive," *Physics of plasmas*, vol. 7, p. 312, 2000.

[20] T. A. Gianakon, "Limitations on the stabilization of resistive tearing modes," *Physics of plasmas*, vol. 8, p. 4105, 2001.

[21] G. Giruzzi *Plasma Phys. Controlled Fusion*, vol. 35, p. A123, 1993.

[22] C. C. Hegna and J. D. Callen, "A closure scheme for modeling rf modifications to the fluid equations," *Physics of plasmas*, vol. 16, no. 11, p. 112501, 2009.

[23] E. D. Held, J. D. Callen, C. C. HEGNA, C. R. Sovinec, T. A. Gianakon, and S. E. Kruger, "Nonlocal closures for plasma fluid simulations," *Physics of plasmas*, vol. 11, no. 5, p. 2419, 2004.

[24] J. J. Ramos, "Fluid and drift-kinetic description of a magnetized plasma with low collisionality and slow dynamics orderings. I. Electron theory," *Physics of plasmas*, vol. 17, no. 8, p. 082502, 2010.

[25] T. Stix, *Waves in Plasmas*. New York, NY: AIP, 1992.

[26] J. S. J. Ramos, "Finite-Larmor-radius kinetic theory of a magnetized plasma in the macroscopic flow reference frame," *Physics of plasmas*, vol. 15, no. 8, p. 082106, 2008.

[27] N. J. Fisch, "Theory of current drive in plasmas," *Reviews of Modern Physics*, vol. 59, p. 175, 1987.

[28] R. W. Harvey and M. McCoy, "The cql3d fokker-planck code," *Advances in Simulation and Modeling of Thermonuclear Plasmas*.

[29] R. Prater, "Heating and current drive by electron cyclotron waves," *Physics of plasmas*, vol. 11, no. 5, p. 2349, 2004.

[30] S. P. Hirshman and D. J. Sigmar, "Neoclassical transport of impurities in tokamak plasmas," *Nucl. Fusion*, vol. 21, p. 1079, 1981.

[31] G. Giruzzi, M. Zabiego, T. A. Gianakon, X. Garbet, A. Cardinali, and S. Bernabei, "Dynamical modelling of tearing mode stabilization by RF current drive," *Nuclear Fusion*, vol. 39, no. 1, pp. 107–125, 1999.

[32] G. S. Nusinovich, O. V. Sinitsyn, L. Velikovich, M. Yeddulla, T. M. Antonsen, A. N. Vlasov, S. R. Cauffman, and K. Felch, "Startup Scenarios in High-Power Gyrotrons," *IEEE Transactions on Plasma Science*, vol. 32, pp. 841–852, June 2004.

[33] N. J. Fisch and A. H. Boozer, "Creating an asymmetric plasma resistivity with waves," *Physical Review Letters (ISSN 0031-9007)*, vol. 45, no. 9, pp. 720–722, 1980.

[34] T. Ohkaway, "Steady State Operation of Tokamaks by RF Heating," *Rep. GA-A-138476, General Atomics, San Diego, CA*, vol. 45, no. 9, 1980.

[35] E. D. Held, J. D. Callen, and C. C. HEGNA, "Conductive electron heat flow along an inhomogeneous magnetic field," *Physics of plasmas*, vol. 10, p. 3933, 2003.

[36] R. W. harvey, "GENRAY," *Bull. Am. Society*, vol. 39, p. 1626, 1994.

[37] B. Barber, "Qhull." `http://qhull.org`, 1995.

[38] C. R. Sovinec, A. H. Glasser, T. A. Gianakon, D. C. Barnes, R. A. Nevel, S. E. Kruger, S. J. Plimpton, A. Tarditi, M. S. Chu, and the NIMROD Team, "Nonlinear magnetohydrodynamics with high-order finite elements," *J. Comp. Phys.*, vol. 195, p. 355, 2004.

[39] D. Shepard, "A two-dimensional interpolation function for irregularly-spaced data," in *Proceedings of the 1968 23rd ACM national conference*, ACM '68, (New York, NY, USA), pp. 517–524, ACM, 1968.

[40] R. J. Renka, "Algorithm 660: Qshep2d: Quadratic shepard method for bivariate interpolation of scattered data," *ACM Trans. Math. Softw.*, vol. 14, pp. 149–150, June 1988.

[41] W. R. Elwasif, D. E. Bernholdt, L. A. Berry, and D. B. Batchelor, "Component framework for coupled integrated fusion plasma simulation," in *Proceedings of the 2007 symposium on Component and framework technology in high-performance and scientific computing*, CompFrame '07, (New York, NY, USA), pp. 93–100, ACM, 2007.

4 Acknowledgements

This work is supported by the SciDAC Center for Simulation of RF Wave Interactions with Magnetohydrodynamics (SWIM), which is funded by the U.S. Department of Energy jointly under under the Fusion Energy Sciences and Advanced Scientific Computing Research programs of the Office of Science, via Cooperative Agreement No. DE-FC02-06ER54899. Computations herein were performed primarily at NERSC, which is also supported by the DoE Office of Science under Contract No. DE-AC02-05CH11231.

We wish to thank C. C. Hegna, J. D. Callen, D. P. Brennan, W. R. Elwasif, and D. B. Batchelor, as well as members of the SciDAC Center for Extended MHD Modeling (CEMM) and the NIMROD and SWIM teams, for useful discussion and feedback.